Chemical Engineering and Processing 72 (2013) 42–50

Contents lists available at ScienceDirect

Chemical Engineering and Processing: Process Intensification

journal homepage: www.elsevier.com/locate/cep

# New prototype for the treatment of falling film liquid effluents by gliding arc discharge part I: Application to the discoloration and degradation of anthraquinonic Acid Green 25

M.R. Ghezzar[a], N. Saïm[a], S. Belhachemi[a], F. Abdelmalek[a,b], A. Addou[a,*]

[a] Laboratoire des Sciences et Techniques de l'Environnement et de la Valorisation, Université de Mostaganem, Algeria
[b] Laboratoire de Spectrochimie LASIR, Université des Sciences et Technologie de Lille 1, Bat C5, Villeneuve d'Ascq, France

ARTICLE INFO

*Article history:*
Received 23 July 2012
Received in revised form 12 April 2013
Accepted 12 June 2013
Available online 20 June 2013

*Keywords:*
Gliding arc discharge treatment
Reactor model
Laminar falling film
Anthraquinonic dye AG 25

ABSTRACT

Gliding arc discharge (GAD) reactors are continuously in progress in order to improve the treatment efficiency of recalcitrant compounds. However, up to now, they remain difficult to transfer to industrial applications because of some technical constraints in their design. In this study, a new efficient prototype is proposed for the treatment of gravity falling film shaped of liquid effluents. The liquid flow rate is now continuous as the tank containing the solution to be treated is replaced by an inclined plate along which flows the liquid. The various working parameters are optimized and the new prototype efficiency is tested on discolouration and degradation of the anthraquinonique Acid Green 25. The optimized values obtained are: the liquid flow rate $\omega = 1\,L\,h^{-1}$, the plate tilt angle $\alpha = 45^{\circ}$ and the channel width $\Delta = 3$ mm. The rates of discolouration and degradation reach 95% and 90% respectively after 12 cycles (180 min) of plasma exposition. The GAD in the presence of humid air generates highly oxidizing radical species such as •OH with a standard potential $E^{\circ}[(^{\bullet}OH/H_2O) = 2.85\,V/SHE]$ and its reducer agent $H_2O_2$ $[E^{\circ}(H_2O_2/H_2O) = 1.68\,V/SHE]$.



## 1. Introduction

The application of water treatments techniques using advanced oxidation processes (AOP) and adaptable to the industrial needs, is a challenge for scientists. Among these techniques, the electric discharges are good alternatives for the treatments of refractory organic pollutants [1–4]. Their advantages being that they generate very reactive in situ species with high oxidizing power.

Many experimental devices have been used in laboratory and proposed for applications at more or less large scale. These devices are characterized by appropriate electrical power supply modes. Among the most utilized techniques, there are (i) the electron beams reactors [5–7]; (ii) the corona discharges [8–10]; (iii) the dielectric barrier discharges (DBD) [11,12]; and (iv) the gliding arc discharges (GAD) [13–20].

Emerging processes using electrical discharges plasma are very often used and applied to various fields. The GAD, i.e., a technique that operates close to ambient temperature and atmospheric pressure, has been successfully applied to the degradation of liquid solutes [14–20] for pollution abatement and for surface treatment in order to obtain high corrosion protection (for example for steels) [21,22]. At first, the previous GAD reactor configuration involved an open cell (GAD I). Then, it has been replaced by a closed reactor (GAD II). But, as it works at discontinuous rate, it is hardly adaptable to industrial applications.

In the presence of humid air the GAD generates highly oxidizing radical species such as •OH with a standard potential $E^{\circ}(OH)/H_2O = 2.85$ V/standard hydrogen electrode. Other species (e.g., •NO and their derivatives, such as peroxynitrite $ONOO^-$) are also formed and participate to the oxidizing character of the plasma $E^{\circ}(ONOO^-/NO_2) = 2.44$ V/standard hydrogen electrode [23].

In this work a new prototype of GAD reactor is developed to be used for the treatment of liquid effluents shaped in falling film. Its efficiency is tested on the discolouration and the degradation of an anthraquinonic dye Acid Green AG25 ($C_{28}H_{20}N_2Na_2O_8S_2$). Working parameters (channel width, flow rate and tilt angle of the plate) values of the new prototype are optimized. Results of the efficiency treatment are compared to those obtained with previous GAD devices.

## 2. Materials and methods

### 2.1. Dye

The Acid Green 25 (AG25) purchased from 'Argos organic' had analytical purity. AG25 is an anthraquinonic dye ($C_{28}H_{20}N_2O_8S_2$,

* Corresponding author at: BP 188, University of Mostaganem, 27000, Algeria. Tel.: +213 45206472; fax: +213 45206472.
*E-mail addresses:* a.addou@univ-mosta.dz, ahmedaddou1@gmail.com (A. Addou).

0255-2701/$ – see front matter © 2013 Elsevier B.V. All rights reserved.
http://dx.doi.org/10.1016/j.cep.2013.06.007

2 Na; $M_m$ = 622 g mol$^{-1}$; $\lambda_{max}$ = 643 nm) and the solutions were prepared using ultra pure distilled water.

### 2.2. Gliding arc discharge apparatus prototypes

#### 2.2.1. GAD I and II

Different configuration of GAD reactor involving the same principle of plasma production have been developed for the treatment of liquids [13,14]. The first reactor (GAD I) consisted in an open thermostated water cooled cylindrical pyrex glass cell of reduced volume (125 mL) containing the liquid sample to be treated by plasma (Fig. 1a).

In order to improve the treatment, the cell was removed and replaced by a thermostated closed reactor able to treat volumes ranging from 180 to 200 mL and using vapor condensation refrigerants. This second device (GAD II) has led to many works (Fig. 1b).

However, these two prototypes have a common disadvantage: they are not applicable to industrial treatments because of (i) the limited volume of liquid that can be treated, (ii) its stationary flow rate, and (iii) the reactor fragility.

#### 2.2.2. Falling film GAD (GAD-FF)

Aiming to have a flexible, easy to use and adaptable method for industrial applications, a new prototype able to treat liquid effluent with continuous flow rate was developed. As it was conceived in order to treat the liquid flow as a laminar film falling by gravity it was denoted GAD-FF (Fig. 1c). The pyrex reactor of GAD I and II was replaced by a stainless steel plate having straight channels of different widths (Fig. 1d). The plate can be inclined from 0 to 90° with respect to the horizontal. It is the site of the absorption reaction between the ionized gas (plasma) and the falling film along the channel. This liquid is pumped from a tank using a peristaltic pump.

The compressed air is driven to a bubbler for saturation with water and goes through an inlet nozzle. An electric arc is produced between two diverging electrodes at a minimum gap (few millimeters) and a suitable voltage difference (around 10 kV). The arc is put away from the ignition point by the feeding gas flow and sweeps along the maximum length of the electrode gap, forming a large plasma plume. A new arc then appears and develops according to the same procedure.

The resulting phase is a plasma at atmospheric pressure and quasi-ambient temperature. It is oriented toward the center of

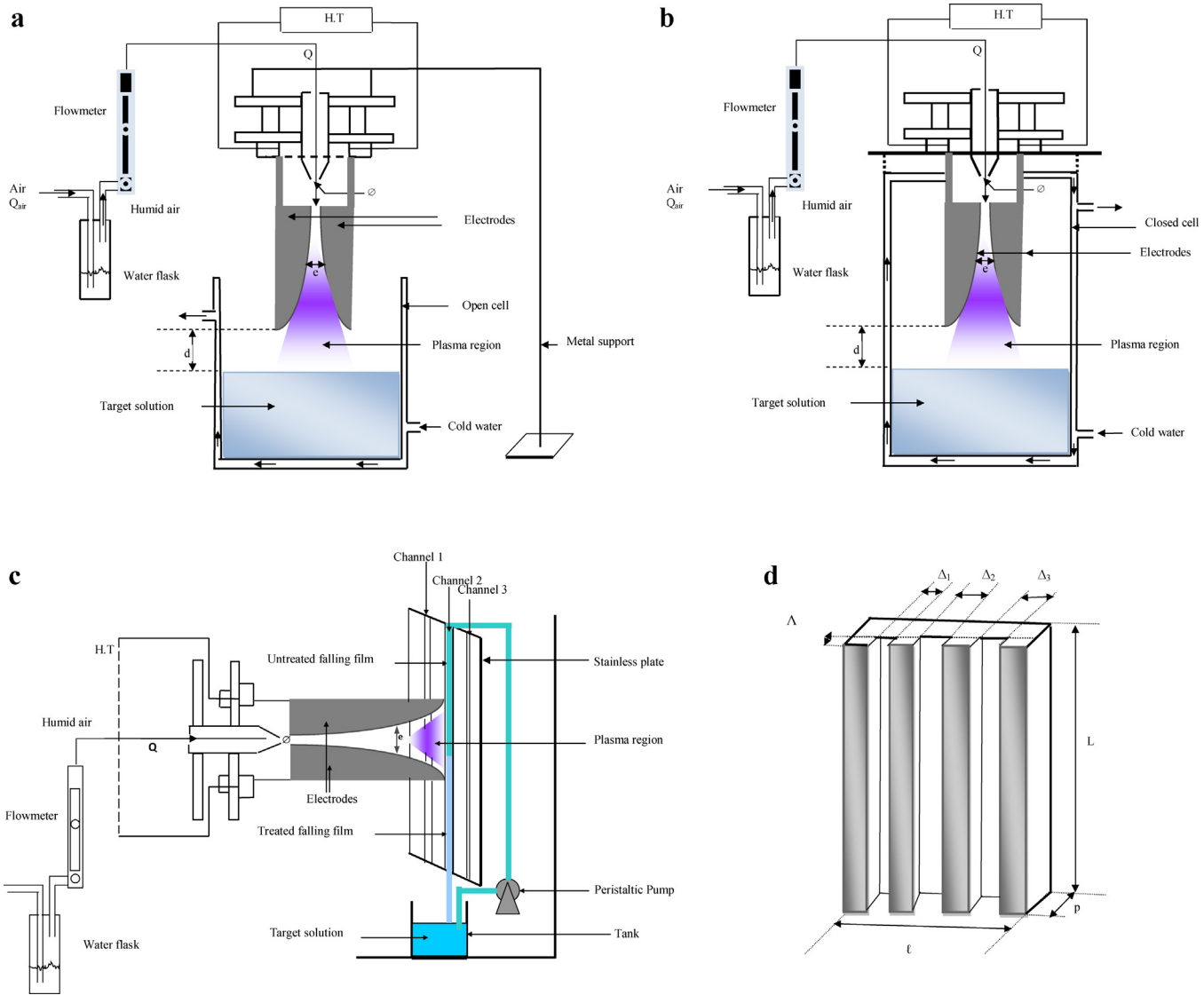


**Fig. 1.** Schemes of the gliding arc discharge GAD: (a) GAD I, (b) GAD II, (c) GAD-FF, and (d) plate-channels.

symmetry of a channel made on a stainless steel plate and licks the liquid falling film along the channel. The plate is set at an angle $\alpha$ with respect to the horizontal and is facing the two electrodes. The recycling of the liquid to be treated is done with a peristaltic pump. The liquid is taken from a tank of variable volume.

#### 2.2.3. Working parameters

*2.2.3.1. Plasma parameters.* Parameters acting on plasma efficiency involved the nozzle diameter of plasma gas ($\Phi$), the inter-electrode distance ($e$), the nature of the plasma gas, the electrode-film distance ($d$) and the gas flow rate ($Q$) and are relevant to all GAD devices at present [13,14]. They were subject to optimization in previous works [14–20] and have been maintained constant in this work.

(i) Diameter of the inlet nozzle of the plasma gas ($\Phi$)The nozzle is directly related to the flux of the plasma gas jet. Its size increases with the active species mobility and the diffusion toward the target to be treated. The inlet nozzle diameter equal to $\Phi$ = 1 mm [13–20].
(ii) Distance inter electrodes ($e$)The plasma plume volume depends on the distance ($e$) between the electrodes and requires to be stable. Such a stability was obtained for $e$ = 3 mm. However, the distance of 5 mm was the distance at which the electric arc is out.
(iii) Plasma gasThe plasma gas used throughout all our works was essentially air saturated with water to minimize the treatment cost and generate active •NO and •OH radicals.
(iv) Distance electrode-film ($d$)Bringing the electrodes nearer to the target leads to a faster diffusion of the species and enables to minimize the treatment time. However, this distance must be relative to the plasma gas rate to insure a regular flow of film inside the channel and to avoid its breaking. In this new reactor configuration, the distance was fixed to 5.5 cm, which is the optimal value enabling a good diffusion of the plasma species and a homogeneous flow along the circulation plate.
(v) Plasma gas flow rate ($Q$)When the rate flow is ranging from 700 to 900 L h$^{-1}$, the characteristic pink color of oxygen plasma can be observed and the reactive plasma species migrate rapidly toward the target to be treated [23,24]. For weaker rates (below 600 L h$^{-1}$), the plume becomes light yellow, characteristic color of nitrogen plasma leading to a slower diffusion. In this work, the gas flow rate was equal to 700 L h$^{-1}$.

*2.2.3.2. GAD-FF parameters.* Parameters added in the frame of GAD-FF development are the plate channel device, the peristaltic pump and the reservoir of the liquid to be treated.

(i) Plate channel device parameters ($\Delta$, $\alpha$)The liquid falling film circulation was performed on a stainless steel plate (length $L$ = 300 mm, width $\ell$ = 150 mm, thickness $\varepsilon$ = 5 mm). This plate is the seat of the plasma-film interaction. It consists of three channels: the length is equal to the one of the plate, the depth is equal to 2 mm and the three channels have different widths $\Delta$ equal to 1, 2, 3 mm respectively (Fig. 1d). The channel provides a homogeneous and regular flow of liquid film. The plate can be tilted by an angle $\alpha$ which varies from 0 to 90° with regard to the horizontal plane.
(ii) Peristaltic pump ($\omega$)The liquid flow is provided by a peristaltic pump whose circulation rate ($\omega$) can be set according to the treatment efficiency.
(iii) Tank volume ($V$)The volume of liquid to be treated is taken from a tank of variable volume and is not limited. In this work, the volume to be treated was maintained equal to 180 mL as this value is identical to the one used in our previous works [13–21] and allows to compare the results. Table 1 summarizes the functional parameters of the different GAD used.

### 2.3. Plasma chemistry

The reactive species of the GAD depend on the plasma gas nature. In the case of humid air, the discharge in ($N_2$–$O_2$–$H_2O$) gives the following products with various concentrations: •OH, •$OH_2$, $O_2$, $H_2$, $H_2O_2$, •H, •O, O, $O_3$, $N_2$, •NO, $NO_2$ $N_2O$ and other excited species resulting from the breaking of O=O and O—OH bonds with relatively weak energies [25,26].

Collision, addition, dissociation and transformation reactions occur, producing molecules which diffuse in the liquid target to be treated. This section summarizes the different species which may be formed and react with the liquid effluent to be treated.

#### 2.3.1. Formation of radicals •OH

The most preponderant species in the GAD of humid air is the radical hydroxyl •OH. It is very reactive and with a single electron has the character of attracting electrons [27,28]. It is a weak acid with a p$K_a$ of 11.9 in the couple •OH/$O^{\bullet -}$. Hydroxyl radicals are known to be entities diffusing poorly with a diffusion coefficient close to $2 \times 10^{-5}$ cm$^2$ s$^{-1}$ [29]. They react nearly where they are produced. They have a strong reactivity on organic compounds [29,30].

Their formation takes place:

(i) Through water vapor which is decomposed by electron collisions following the reaction [30]:

$$H_2O + e^- \rightarrow {}^{\bullet}OH + {}^{\bullet}H + e^- \quad (R1)$$

(ii) By collision with atomic oxygen O:

$$H_2O + O \rightarrow 2{}^{\bullet}OH \quad (R2)$$

(iii) By $H_2O_2$ photon absorption:

$$H_2O_2 + h\upsilon \rightarrow 2{}^{\bullet}OH \quad (R3)$$

(iv) By decomposition of ozone by hydrogen peroxide:

$$O_3 + H_2O_2 \rightarrow {}^{\bullet}OH + O_2 + HO_2^{\bullet} \quad (R4)$$

$$OH_2^{\bullet} + O_3 \rightarrow {}^{\bullet}OH + 2O_2 \quad (R5)$$

(v) Formation of oxygenated water [30,31]
(vi) Hydrogen peroxide $H_2O_2$ can be formed at low temperature in the GAD.
(vii) By combination of •OH:

$${}^{\bullet}OH + {}^{\bullet}OH \rightarrow H_2O_2 \quad (R6)$$

(viii) By combination of $HO_2^{\bullet}$

$$HO_2^{\bullet} + HO_2^{\bullet} \rightarrow H_2O_2 + O_2 \quad (R7)$$

(ix) By dissociation and recombination:

$$2HO_2^{\bullet} \rightarrow H_2O_2 + O_2 \quad (R8)$$

#### 2.3.2. Formation of reactive nitrogen species

Since the dissociation energy of nitrogen is high, the molecules of $N_2$ being in an excited state can interact with atomic oxygen to give •NO [26,31–33].

(i) Dissociation of $N_2$ with one excited electron:

$$N_2 + e^- \rightarrow N + N + e^- \quad (R9)$$

(ii) Transfer of excitation and recombination state:

$$N + {}^{\bullet}OH \rightarrow NO + H \quad (R10)$$

**Table 1**
Functional parameters for three devices of gliding arc discharge.

| Functional parameters | Gliding arc discharge (GAD) | | |
|---|---|---|---|
| | GAD I | GAD II | GAD- FF |
| Nozzle diameter ϕ (mm) | 2 | 1 | 1 |
| Distance inter electrode *e* (mm) | 3 | 3 | 3 |
| Distance electrode-film *d* (cm) | 5 | 5 | 5.5 |
| Humid air flow rate *Q* ($L\,h^{-1}$) | 975 | 700–900 | 700 |
| Circulation rate *ω* ($L\,h^{-1}$) | 0 | 0 | 1 |
| Thickness of the transfer layer *δ* (mm) | 40 | 40 | 2 |
| Volume to be treated (mL) | 125 | From 180 to 300 | Not limited |
| Electrical circuit | 9000 V–100 mA | 9000 Volts-100 mA | 9000 V–100 mA |
| Nature of the reactor | Pyrex glass. Open device | Pyrex. Glass Closed device | Steel plate |
| Discharge disposal | Vertical | Vertical | Horizontal |
| Nature of the flow | Stationary | stationary | Non stationary |
| Angle of inclinaison of the plate (°) | | | 45 |
| Width of the slot (mm) | – | – | 3 |
| Cooling | With | With | Without |
| Shape of the target liquid | Cylindrical | Cylindrical | Falling Film |

(iii) Dissociation and recombination of $N_2$

$$N_2 + O^\bullet \rightarrow {}^\bullet NO + N^\bullet \quad (R11)$$

(iv) By oxidation of nitrogen:

$$N_2 + O_2 \rightarrow 2{}^\bullet NO \quad (R12)$$

(v) Conversion of NO:

$$NO + {}^\bullet OH \rightarrow HNO_2 \quad (R13)$$

(vi) Dissociation of $HNO_2$ in aqueous medium:

$$HNO_2 \rightarrow H^+ + NO_2^- \quad (R14)$$

(vii) Transformation to $NO_2$ by •OH:

$$HNO_2 + {}^\bullet OH \rightarrow NO_2 + H_2O \quad (R15)$$

(viii) Conversion of $NO_2$ and dissociation of $HNO_3$ in aqueous medium:

$$NO_2 + {}^\bullet OH \rightarrow HNO_3 \rightarrow H^+ + NO_3^- \quad (R16)$$

*2.3.3. Reactions between NO and the radicals •OH and $HO_2^\bullet$*

Peroxynitrite ion is suspected to be a supplementary oxidant playing an important role in the treatments by GAD [34–36]. It is an isomer of nitric acid obtained by action of nitrogen species and hyper oxide ion $O_2^{\bullet -}$.

$$NO + {}^\bullet OH \rightarrow HNO_2 \quad (R17)$$

$$NO + O_2^{\bullet -} \rightarrow ON - O_2^- \quad (R18)$$

The peroxinitrous acid can be dissociated into $NO_2$ and •OH or become an isomer of nitric acid [36–38].

$$ON - O_2H + H_2O \leftrightarrow ON - O_2^- + H_3O^+ \quad (R19)$$

$$ON - O_2H \leftrightarrow NO_2 + {}^\bullet OH \quad (R20)$$

$$ON - O_2H \rightarrow HNO_3 \quad (R21)$$

Table 2 shows the standard potential values of some redox couples present in the GAD of humid air [39].

## 2.4. Analysis

A known quantity of AG25 was dissolved in 180 mL of distilled water in order to obtain a 80 μM solution. The treatment of aqueous film was done in 12 cycles accomplished in a theoretical time calculated according to Eq. (1).

$$t\,(\text{min}) = 60 \times \frac{V\,(\text{L})}{\omega\,(\text{L h}^{-1})} \quad (1)$$

For 180 mL of the AG25 (80 μM) and a circulation rate of 1 $L\,h^{-1}$, the theoretical circulation time for a cycle was equal to 10.8 min. However, the experiments showed that this time can reach 15 min. This difference is due to the different nature of the liquids to be treated (solutions, solvents, etc.) which have different physicochemical characteristics (molar mass, density, concentration, etc.) implying a circulation time proper to each fluid. Consequently, a time of 15 min was retained to define the real duration of a treatment cycle by GAD-FF ($t_{cycle}$ = 15 min).

The samples of AG25 (80 μM) were analyzed by UV/visible spectroscopy (double beam OPTIZEN 2021 spectrophotometer) in a range of wavelength ranging from 200 to 700 nm. This analysis consisted of tracking the discolouration as a function of the exposition time (number of cycles) to the plasma. The AG25 concentration of each treated sample was determined at the maximum absorption wavelength ($\lambda_{max}$ = 643 nm, [0,100 μM], $\varepsilon$ = 88.600 $cm^{-1}\,mol^{-1}\,L$) using a calibration curve. In parallel, the degradation was evaluated by measuring the chemical demand of oxygen (DCO), using the method of potassium dichromate according to the standard procedure AFNOR NFT 90-102 [40].

The discolouration (DEC) and the degradation (DEG) rates were calculated by formulae (2) and (3) respectively:

$$\%DEC = \left(1 - \frac{C}{C_0}\right) \times 100 \quad (2)$$

**Table 2**
Standard potential values of some redox couples present in the GAD of humid air.

| Ox + ne⁻ | ↔ | Red | $E^\circ$ (V/ENH) |
|---|---|---|---|
| $^\bullet OH + H^+ + e^-$ | ↔ | $H_2O$ | 2.85 |
| $H^+ + ON - OO^- + e^-$ | ↔ | $NO_2^- + {}^\bullet OH$ | 2.44 |
| $O_{gas} + 2H^+ + 2e^-$ | ↔ | $H_2O$ | 2.42 |
| $O_3 + 2H^+ + 2e^-$ | ↔ | $O_2 + H_2O$ | 2.07 |
| $^\bullet OH + e^-$ | ↔ | $OH^-$ | 2.02 |
| $HO_2^\bullet + 3H^+ + 3e^-$ | ↔ | $2H_2O$ | 1.70 |
| $H_2O_2 + 2H^+ + 2e^-$ | ↔ | $2H_2O$ | 1.68 |
| $O_3 + 2H^+ + 2e^-$ | ↔ | $3H_2O$ | 1.51 |
| $HO_2^\bullet + 6H^+ + 6e^-$ | ↔ | $H_2O_2$ | 1.50 |
| $O_2 + 4H^+ + 4e^-$ | ↔ | $2H_2O_{(liq)}$ | 1.23 |
| $NO_2 + H^+ + e^-$ | ↔ | $HNO_2$ | 1.09 |
| $NO_2 + 2H^+ + 2e^-$ | ↔ | $NO + H_2O$ | 1.05 |
| $NO_3^- + 3H^+ + 2e^-$ | ↔ | $HNO_2 + H_2O$ | 0.96 |
| $NO_3^- + 4H^+ + 3e^-$ | ↔ | $NO + 2H_2O$ | 0.92 |

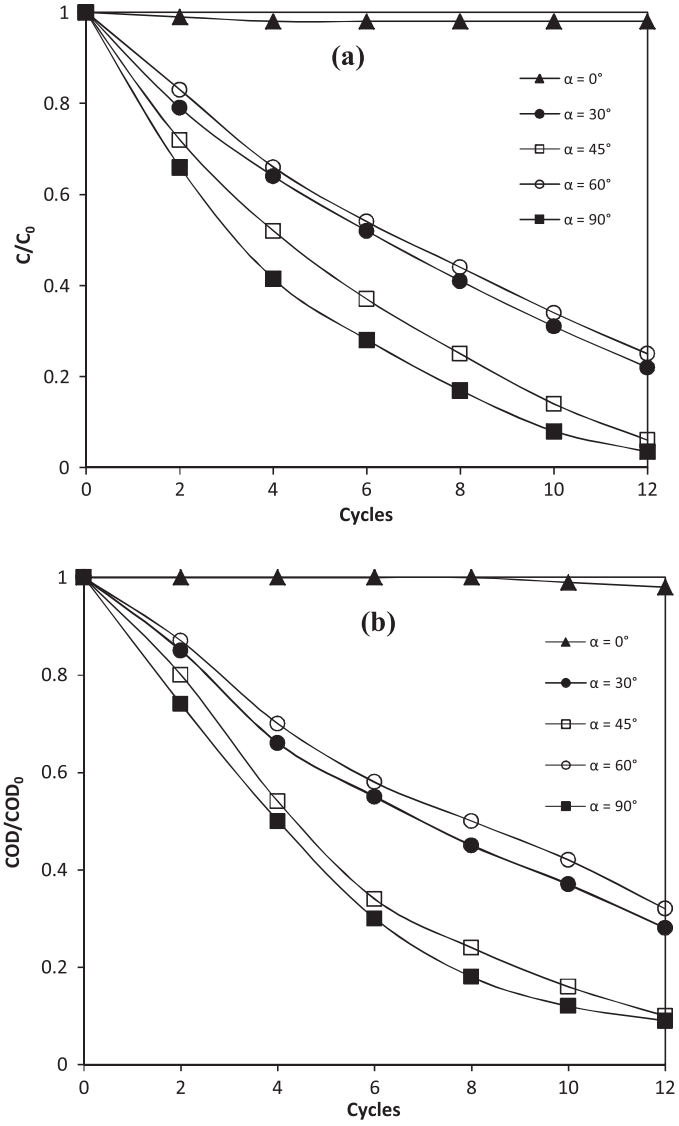


**Fig. 2.** Discolouration (a) and degradation (b) versus treatment time (number of cycles) and inclination angles: $\omega = 1\,L\,h^{-1}$, $\Delta = 3\,mm$, $d = 5.5\,cm$, $V = 180\,mL$, $Q_{air} = 700\,L\,h^{-1}$.

and

$$\%DEG = \left(1 - \frac{COD}{COD_0}\right) \times 100 \quad (3)$$

where $C_0$: AG25 concentration at time $t = 0$; $C$: AG25 concentration at time $t$; $COD_0$: AG25 COD at time $t = 0$; $COD_0$: AG25 COD at time $t$.

## 3. Results and discussion

### 3.1. Optimization of plasma parameters

#### 3.1.1. Influence of the tilt angle ($\alpha$)

The influence of the tilt angle ($\alpha$) of the plate on the treatment was studied by circulating the AG25 solution on the channel $\Delta_3 = 3\,mm$ (Fig. 1d) by maintaining the circulation rate constant at $\omega = 1\,L\,h^{-1}$. The inclination angle ($\alpha$) was varied from 0 to 90° with respect to horizontal plane. The results obtained for the discolouration and the DCO versus the number of cycles are shown in Fig. 2.

For 12 treatment cycles, the rates of discolouration and degradation are (95 and 90%) for $\alpha = 45°$ and (96 and 91%) for $\alpha = 90°$.

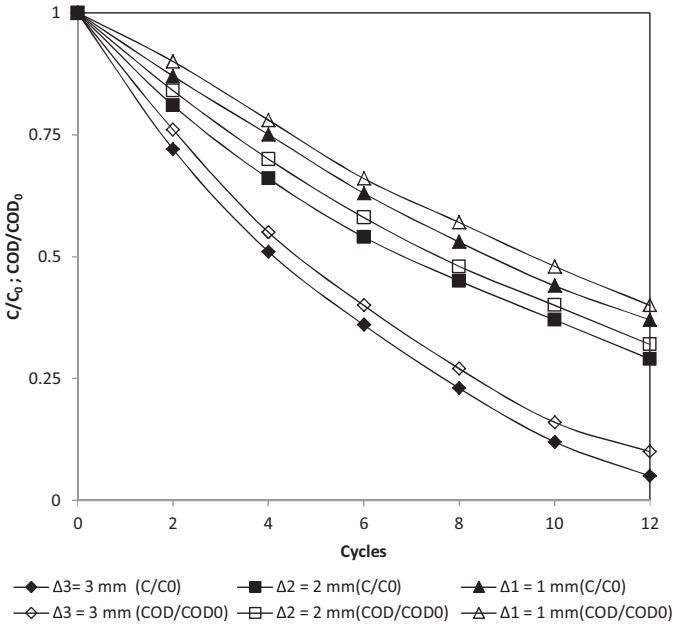


**Fig. 3.** Discolouration and degradation versus treatment time (number of cycles) and width of channels: $\omega = 1\,L\,h^{-1}$, $\alpha = 45°$, $d = 5.5\,cm$, $V = 180\,mL$, $Q_{air} = 700\,L\,h^{-1}$, $\Delta_i = 1\,mm$.

These values are more important than those obtained at the plate inclination of 30° (72 and 70%) and 60° (70 and 68%). For the horizontal position set at $\alpha = 0°$, no significant discolouration or degradation occurred, which is predictable given the absence of contact between the plasma and the film.

The vertical position ($\alpha = 90°$) gives an efficiency comparable to the medium position relative to $\alpha = 45°$. However, the observations showed that the position set at this angle ($\alpha = 45°$) produces a greater stability of the film and induces a synergy between the flow and plasma plume. However, at the vertical position of the plate ($\alpha = 90°$) some streams appear generating dry regions in the channel. Consequently, the treated zone becomes smaller than the available exchange area.

The choice of the contact angle must not only take into account the efficiency of the pollutant elimination, but also some observations during the experiments. From this work, it is more judicious to realize the treatments at the position $\alpha = 45°$ for the following reasons: (i) the liquid film is stable; (ii) the more important contact surface enables to treat a big part of the film, and (iii) a great lifetime of the pump with respect to the vertical position which requires a considerable driving force. Works done by Maron et al. [41]** on the wetting and the breaking of water liquid films on an inclined plate revealed that an inclination angle between 0 and 45° was more advantageous for the traditional falling film process. In emerging processes, and more especially in the study about coupling between the gas absorption by a liquid and the distillation to treat COV, it was also noticed that an inclination angle equal to 45° was technically more suitable for an industrial extrapolation of the process and cheaper [42].

#### 3.1.2. Influence of the channel width $\Delta$

The circulation rate of the solution of AG25 was always maintained equal to $\omega = 1\,L\,h^{-1}$ and the inclination angle was fixed at 45°, only the channel width $\Delta$ was variable. The discolouration variations of AG25 and the evolution of COD versus treatment time for different widths $\Delta$, are shown in Fig. 3.

The results show that the best treatment was obtained with the channel width corresponding to $\Delta_3 = 3\,mm$. Indeed, discolouration and degradation rates were respectively equal to 95 and 90%

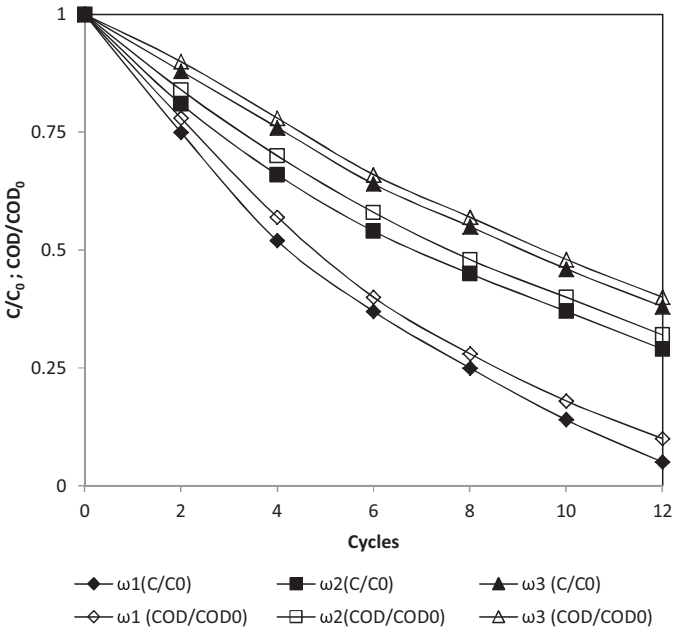


**Fig. 4.** Discolouration and degradation versus treatment time (number of cycles) and circulation velocities: $\alpha = 45^\circ$, $\Delta = 3$ mm, $d = 5.5$ cm, $V = 180$ mL, $Q_{air} = 700\,L\,h^{-1}$, $\omega_i = 1\,L\,h^{-1}$.

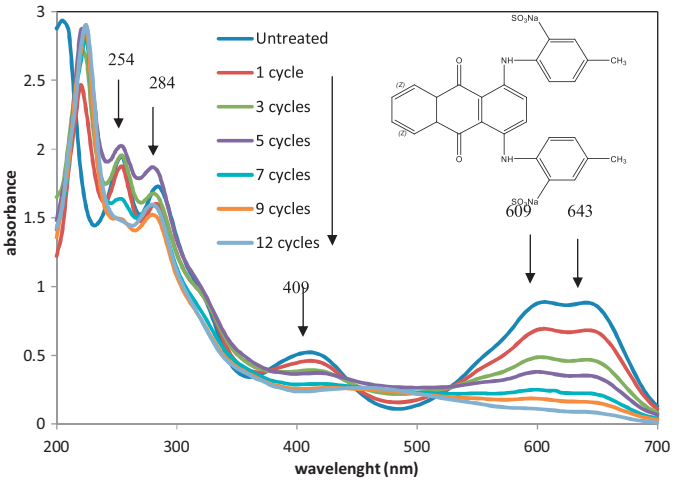


**Fig. 5.** Chemical structure of the AG25 and UV/visible spectra of the AG25 versus number of cycles: $\alpha = 45^\circ$, $\omega = 1\,L\,h^{-1}$, $\Delta = 3$ mm, $d = 5.5$ cm, $Q_{air} = 700\,L\,h^{-1}$, $V = 180$ mL.

for $\Delta_3 = 3$ mm, 71 and 68% for $\Delta_2 = 2$ mm then 63 and 60% for $\Delta_1 = 1$ mm.

These results could be explained by the fact that the wider the film is, the thinner it is. So, it is more stabilized and easy to canalize through the channel. This leads to an intensification of matter transfer between the ionized gas (plasma) and the aqueous film. During the experiments, it was noticed that a triangular liquid front get formed randomly whatever the channel width, and this during the first seconds from the start of the liquid circulation. Nevertheless, for the narrowest channels $\Delta_1$ and $\Delta_2$, this aspect lasts longer causing the film tearing. Ryu et al. [43] have shown that the dimensions of the micro channels affect the efficiency of the process of gas absorption by a falling liquid film. The study showed that the greater the channel width is and the better the gas absorption by the liquid will be. This leads to a more significant transfer on the contact surface.

### 3.1.3. Influence of the circulation rate $\omega$

The inclination angle of the plate was fixed at 45° and the liquid film flew through channel 3 mm width. Influence of liquid circulation rate was studied as a function of treatment time. The discolouration and the DCO rates are shown in Fig. 4. Results show that more the liquid circulation rate is slow, better is the treatment. For $\omega_1 = 1\,L\,h^{-1}$, the discolouration and the degradation rates reach 95 and 90% respectively; for $\omega_2 = 2\,L\,h^{-1}$, they are of the order of 70 and 68% and for $\omega_3 = 3\,L\,h^{-1}$ they decrease to reach 68 and 60%.

It is likely that the liquid circulation rate affects the transfer speed of plasma radical reactive species in the aqueous film. Indeed, more circulation rate is high, more contact between the two phases is fast and less diffusion of reactive species in the liquid treat will be important. This is confirmed by the work of Zanfir and Gavrilidis [44] who explain that the matter transfer can take place in a zone other than the one of aqueous phase. So, more circulation rate is high and more the reactive species transfer can be done toward the plate and not toward the film, explaining the decrease of the treatment efficiency.

## 3.2. Study of the AG25 treatment by GAD-FF

### 3.2.1. Study of the discolouration

Fig. 5 shows UV/visible spectra of the AG25 treated in the new prototype as a function of plasma exposition time. The structure of the studied molecule is also indicated. The spectrum UV/visible of the untreated AG25 shows that the colorant presents absorption bands both in visible and UV regions. It is characterized by a double band in the visible region whose maximum absorption corresponds to 609 and 643 nm and a band located at 409 nm. They are attributed to anthraquinonic group of the colorant molecule. The bands in the UV region are located at 254 and 284 nm and are respectively attributed to benzenic cycles and to those substituted by the $SO_3^-$ groups.

The absorption bands located in the visible part of the spectrum decrease in intensity versus the number of cycles, and an important reduction is in particularly observed the peak intensity of the AG25 located at 643 nm, giving evidence for the degradation of chromophore, responsible for the color of AG25 molecule. At the same time, the studied UV spectrum shows an increase of the absorption peaks intensity at 254 and 284 nm. This trend explains the probable production of aromatic cycles present in the original molecule of AG25 [18,45–47]. This last stage of cycles opening is a slow and difficult process to conceive.

The results give evidence for the oxidizing effect of hydroxyl radicals •OH on the active sites of the AG25 molecule in the aqueous film. These radicals are of non selective nature toward molecules to be degraded [48]. The discolouration reflects the concentration decrease of the studied molecule and a probable degradation of the colorant solution.

Fig. 6 shows the evolution of AG25 concentration in solutions treated with the three configurations of GAD.

The plasma reaction takes place between the AG25 molecules and the majority plasma species •OH and •NO [23,24]. This leads to the kinetic law given by Eq. (4)

$$-\frac{dC}{dt} = kC\,[^{\bullet}OH]\,[^{\bullet}NO] \tag{4}$$

where $k$: rate constant ($min^{-1}$); $t$: treatment time (min); $^{**}C$: dye concentration (μM); [•OH]: •OH concentration (μM); [•NO]: •NO concentration (μM).

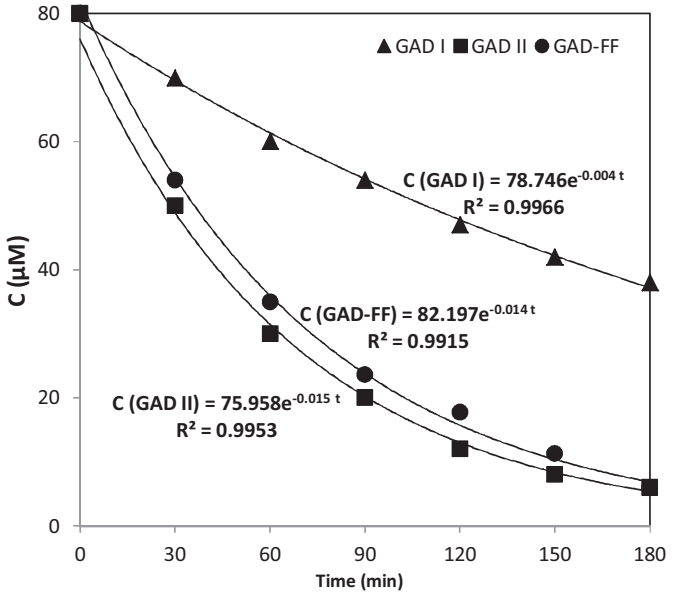


**Fig. 6.** Evolution of AG25 concentration versus treatment time for the three configurations: $\alpha = 45°$, $\omega = 1\,L\,h^{-1}$, $\Delta = 3$ mm, $d = 5.5$ cm, $Q_{air} = 700\,L\,h^{-1}$, $V = 180$ mL.

The •OH and •NO flux driven by the plasma gas being constant, implies the constancy of term $k[•NO][•OH] = k_{app}$. Eq. (4) will be written as Eq. (5):

$$-\frac{dC}{dt} = k_{app}C \tag{5}$$

The integration of 6 gives Eq. (5):

$$C = C_0 e^{-k_{app}t} \tag{6}$$

$k_{app}$: apparent rate constant ($min^{-1}$).

The discolouration reaction follows the kinetic law of pseudo first order proved by Eqs. (4)–(7).

Table 3 gives the different efficiencies of discolouration, the respective rate constants and the plasma gas flow rates for the different configurations of GAD. For 180 min of treatment, the discolouration reached 96 and 95% respectively in GAD II and GAD-FF with rate constants of 0.0015 and 0.014 $min^{-1}$. These results show that the efficiency of GAD-FF is comparable to the one of GAD II. However, it must be noted that the first works with a plasma gas rate of 700 $L\,h^{-1}$ while the second operates with a more important one, equal to 900 $L\,h^{-1}$.

The GAD I reactor gave the lowest efficiency with only 49% of discolouration rate and a rate constant of 0.04 $min^{-1}$. Without cover in the GAD I, the plasma species get dispersed rather in ambient air than in the liquid target, explaining the weak efficiency.

**Table 3**
AG25 discolouration and degradation parameters for three devices of GAD.

| GAD prototypes | GAD I | GAD II | GAD-FF |
|---|---|---|---|
| Discolouration (%) | 49 | 96 | 95 |
| $k_{app}^{DEC}$ ($min^{-1}$) | 0.004 | 0.015 | 0.014 |
| Degradation (%) | 40 | 91 | 90 |
| $k_{app}^{DEG}$ ($min^{-1}$) | 0.003 | 0.01 | 0.01 |
| Gas flow rate ($L\,h^{-1}$) | 900 | 900 | 700 |
| Residence time (min) | 180 | 180 | 180 |
| Energy consumption (kWh/0.0498 g of AG25) | 1.2 | 1.2 | 1.2 |
| Energy cost (€)/1 g of AG25 | 2.34[a] | 2.34[b] | 2.34[b] |
| Specific mass consumption (SMC) (kWh/1 g of AG25) | 134 | 134 | 134 |

[a] For only 40% of degradation.
[b] For 90% of degradation.

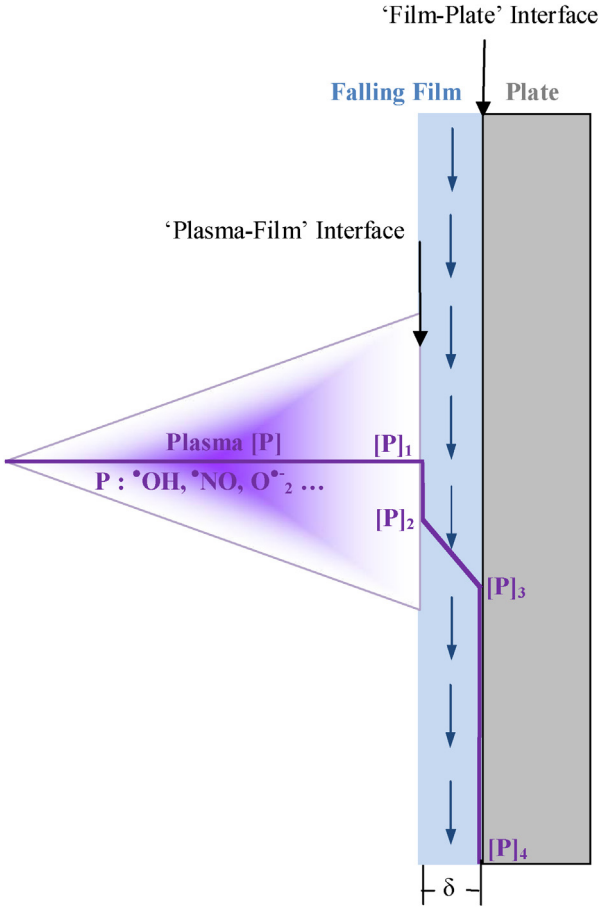


**Fig. 7.** Scheme of interfacial transfer 'Plasma-Film'.

To interpret physically these results, it would be interesting to focus the study on the plasma species migration toward the aqueous target with the different Glidarc. This migration can be explained by a mechanism of transfer phenomenon inspired from the double film model of Lewis and Whitman [49]. The mechanism involved, shown Fig. 7, is the interfacial transfer between the plasma jet containing mainly •OH, $OH_2^•$, $O_2^{•-}$, •NO species and the liquid target. According to this theory, the transfer resistance of a plasma species $P$ is entirely located at the plasma–liquid interface. Once the active species cross this layer, it diffuses in the film whose thickness noted $\delta$ is equal to the depth of the plate channel $\Lambda$ (Fig. 1d). In this work it is equal to 2 mm in order to maximize the migration of oxidizing species in the liquid part. On the opposite, in the GAD I and GAD II reactors, the thickness $\delta = 40$ mm (Table 1) is equal to the liquid depth having a cylindrical shape. This thickness, 20 times more important than the liquid film, implies a bad diffusion of active species and slows down the migration speed of plasma species in the liquid phase. The Fig. 7 shows the concentrations of a plasma specie $P$ for the different cases.

[P]: concentration of a plasma specie in the plasma (ionized gas);
$[P]_1$: concentration of a plasma specie in the plasma-film interface;
$[P]_2$: concentration of a plasma specie in the film;
$[P]_3$: concentration of plasma specie in the film-plate interface;
$[P]_4$: concentration of the plasma specie downstream the film.

According to the double film theory: $[P] < [P]_1 < [P]_2 < [P]_3 < [P]_4$. This decreasing sequence of the plasma species concentration confirms the idea that more important the thickness of the transfer

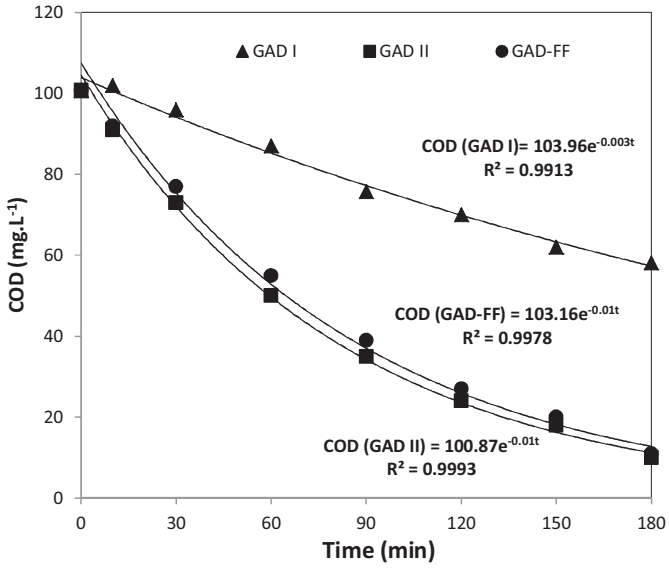


**Fig. 8.** Evolution of COD versus treatment time for the three GAD configuration: $\alpha = 45^\circ$, $\omega = 1\ L\ h^{-1}$, $\Delta = 3$ mm, $d = 5.5$ cm, $Q_{air} = 700\ L\ h^{-1}$, $V = 180$ mL.

layer is, more important is a resistance against the plasma diffusion. From this fact, there will be less plasma species P able to react with active sites of the molecule for GAD I and GAD II.

*3.2.2. Study of the AG25 degradation*

Different works [13–20] showed that the treatment by GAD is interpreted not only as the breaking of the chromophore responsible for the color, but also by the fragmentation of organic molecules in favor of the formation of other smaller and less harmful molecules [50]. This phenomenon commonly called degradation may be quantified by measuring the chemical demand in oxygen (COD) of effluents treated by plasma. In the case of total degradation of AG25; $CO_2$ and the mineral compounds are obtained according to the following the reaction:

$$C_{28}H_{20}N_2O_8S_2Na_2 + 35O_2 \rightarrow 28CO_2 + 2NO_3^- + 4H^+ + 2SO_4^{--} + 2Na^+ + 8H_2O \quad (22)$$

Fig. 8 illustrates the variation of the COD of AG25 (80 μM) solutions as a function of treatment time in the reactors GAD I, GAD II and GAD-FF. The curves obtained show kinetics of pseudo-first order as it is the case for discolouration.

Table 3 summarizes the degradation rates, the rate constants corresponding to this phenomenon and the plasma gas rates used for each plasma reactor. For a treatment during 180 min the degradation rates reach 91 and 90% respectively for GAD II and GAD-FF with an identical rate constant of 0.01 $min^{-1}$. Here also, the same efficiency as in the utilization of GAD II is obtained. The degradation is interpreted by an important fall of COD of aqueous solutions. This is due to the very high oxidation potential of plasma.

The general degradation mechanism involves the previous addition of •OH and •NO radicals on unsaturated bonds.

Saquib and Muneer [51] degrade Acid Green 25 by $TiO_2$/UV process and proposed probable pathways of degradation. The degradation products were analyzed by gas chromatography–mass spectrometry (GC–MS).

Acid Green 25, upon the transfer of an electron, can form radical anion, which may undergo addition of a hydroxyl radical followed by ring cleavage to give the keto acid. Intermediate product may undergo ring cleavage followed by abstraction of a proton to give keto acid. This product, on transfer of an electron followed by addition of a hydroxyl radical, may lose the phenyl ring to give the dicarboxylic acid.

The product, upon the transfer of an electron, can form the radical cation, which may undergo cleavage to give other probable fragmentation products. The formation of 4-aminonaphthalene sulphonic acid could also occur.

The radical species generated by the wet air GAD [50,52] such as •OH, $^{\bullet}O_2H$, O•, $O_2^{\bullet -}$, O• occur in the process of discolouration and degradation of AG25. These species in solution allow the formation of other oxidizing and acidifying substances which improve the efficiency of treatment such as $H_2O_2$ formed from the equations:

$$2^{\bullet}OH \leftrightarrow H_2O_2 \quad (23)$$

$$2HO_2^{\bullet} \leftrightarrow H_2O_2 + O_2 \quad (24)$$

$$O^{\bullet} + O_2 + M \leftrightarrow O_3 + M \quad (25)$$

By diffusion in the liquid effluent to be treated, the nitrogen species can form peroxynitrite:

$$O^- + NO_2^{\bullet} \rightarrow ONOO^- \quad (26)$$

$$OH^{\bullet} + NO_2^{\bullet} \rightarrow ONOOH \quad (27)$$

The peroxynitrite is known as an oxidizing agent rather strong ($E^\circ(ONOO^-/NO_2^-) = 2.44$ V/SHE) and able to participates to the degradation process of organic pollutants [23,50].

## 4. Energy consumption

In order to evaluate the energy consumption, an electrical counter was placed on GAD I, GAD II and GAD-FF apparatus. The energy consumed was a linear function of time treatment and was estimated to 1.2 kWh for 180 min.

The AG25 solution contains 8.96 mg of solute in 180 mL of water in order to obtain, a concentration of 80 μM. We can theoretically calculate the specific mass consumption (SMC) of the plasma process that is of 1.2 kWh/0.00896 g(AG 25) = 134 kWh/1 g of AG 25 with a cost of 238 DZD (Algerian Dinar) equivalents to 2.30 €.

It should be noticed that the three devices GADI, GAD II and GAD-FF consume the same energy cost to treat the AG25 dye, since the treatment time is the same (180 min), but the degradation rates differ (40% for GAD I, 90% for GAD and II GAD-FF).

## 5. Conclusion

A new prototype of treatment of liquid effluents by gliding arc discharge is developed and described. The liquid is treated in film shape falling by gravity through a channel of known width and circulating along a stainless steel plate which can be inclined from 0 to 90° with respect to horizontal plane. A first application implying the treatment of an AG 25 solution versus exposure time to the discharge is shown. The results obtained are of the same order of magnitude as those found with the GAD II in previous work.

The new device GAD-FF has been developed in order to intensify the process of gliding discharge and to improve effluents treatment under continuous rate and more especially to promote the implementation of this prototype in industry.

The optimized working parameters of this new prototype for a maximum yield are as follow:

- Inclination angle of the plate $\alpha = 45^\circ$;
- Circulation rate of liquid film $\omega = 1\ L\ h^{-1}$;
- Width of the channel $\Delta = 3$ mm;
- Plasma gas flow $Q = 700\ L\ h^{-1}$.

With the help of the new design of Glidarc studied in this work, the process can be extrapolated to pilot and/or industrial scale. Works coupling the new GAD prototype with $TiO_2$ particles in order to intensify the plasma process are now in progress.

## References


[1] F. Alshamsi, A. Albadwawi, A.S. Alnuaimi, M.M. Rauf, M.A.S.S. Ashraf, Comparative efficiencies of the degradation of Crystal Violet using UV/hydrogen peroxide and Fenton's reagent, Dyes and Pigments 74 (2007) 283–287.

[2] E. Bizani, K. Fytianos, I. Poulios, V. Tsiridis, Photocatalytic decolorization and degradation of dye solutions and wastewaters in the presence of titanium dioxide, Journal of Hazardous Materials 136 (2006) 85–94.

[3] M. Catanho, G.R.P.J. Malpass, A. Motheo, Photoelectrochemical treatment of the dye reactive red 198 using DSA® electrodes, Applied Catalysis B: Environmental 62 (2006) 193–200.

[4] G. Chen, M. Zhou, S. Chen, W. Chen, The different effects of oxygen and air DBD plasma by products on the degradation of methyl violet 5BN, Journal of Hazardous Materials 172 (2009) 786–791.

[5] K. Kawamura, S. Aoki, H. Kimura, K. Adachi, T. Katayama, K. Kengaku, Y. Sawada, Pilot plant experiment on the treatment of exhaust gas from a sintering machine by electron beam irradiation, Environmental Science & Technology 14 (1980) 288–293.

[6] P.M. Penetrante, M.C. Hsiao, J.N. Bardsley, B.T. Merritt, G.E. Vogtlin, A. Kuthi, C.P. Burkhart, J.R. Bayless, Identification of mechanisms for decomposition of air pollutants by non-thermal plasma processing, Plasma Sources Science and Technology 6 (1997) 251–259.

[7] B.M. Penetrante, M.C. Hsiao, B.T. Merritt, G.E. Vogtlin, P.H. Wallman, Comparison of electrical discharge techniques for nonthermal plasma processing of NO in $N_2$, IEEE Transactions on Plasma Science 23 (1995) 679–687.

[8] R.H. Amirov, J.O. Chae, Y.N. Desserieterik, E.A. Filimanova, M.B. Zhelezniak, Removal of $NO_x$ and $SO_2$ from air excited by streamer corona: experimental results and modeling part 1, Japanese Journal of Applied Physics 37 (1998) 3521–3530.

[9] W. Wang, J. Zhang, F. Liu, Y. Liu, Y. Wang, Study on density distribution of high-energy electrons in pulsed corona discharge, Vacuum 73 (2004) 333–339.

[10] K. Yan, T. Yamamoto, S. Kanazawa, T. Ohkubo, Y. Nomoto, J.S. Chang, Control of flow stabilized positive corona discharge modes and NO removal characteristics in dry air by $CO_2$ injections, Journal of Electrostatics 46 (1999) 207–219.

[11] B. Lu, X. Zhang, X. Yu, T. Feng, S. Yao, Catalytic oxidation of benzene using DBD corona discharges, Journal of Hazardous Materials 137 (2006) 633–637.

[12] F. Huang, L. Chen, H. Wang, T. Feng, Z. Yan, Degradation of methyl orange by atmospheric DBD plasma: analysis of the degradation effects and degradation, Journal of Electrostatics 70 (2012) 43–47.

[13] H. Lesueur, A. Czernichowski, J. Chapelle, French Patent 2,639,172 (1988).

[14] F. Abdelmalek, S. Gharbi, B. Benstaali, A. Addou, J.L. Brisset, Plasmachemical degradation of azo dyes by humid air plasma: Yellow Supranol 4 GL, Scarlet Red Nylosan F3 GL and industrial waste, Water Research 38 (2004) 2339–2347.

[15] F. Abdelmalek, M.R. Ghezzar, M. Belhadj, A. Addou, J.L. Brisset, Bleaching and degradation of textile dyes by nonthermal plasma process at atmospheric pressure, Industrial & Engineering Chemistry Research 45 (2006) 23–29.

[16] F. Abdelmalek, R.A. Toress, E. Combet, C. Petrier, C. Pulgarin, A. Addou, Gliding arc discharge (GAD) assisted catalytic degradation of bisphenol A in solution with ferrous ion, Separation and Purification Technology 63 (2008) 30–37.

[17] A. Doubla, L. Bouba Bello, M. Fotso, J.L. Brisset, Plasmachemical decolourisation of bromothymol blue by gliding electric discharge at atmospheric pressure, Dyes and Pigments 77 (2008) 118–124.

[18] M.R. Ghezzar, F. Abdelmalek, M. Belhadj, N. Benderdouche, A. Addou, Gliding arc plasma assisted photo-catalytic degradation of anthraquinonic acid green 25 in solution with $TiO_2$, Applied Catalysis B: Environmental 72 (2007) 304–313.

[19] M.R. Ghezzar, F. Abdelmalek, M. Belhadj, N. Benderdouche, A. Addou, Enhancement of the bleaching and degradation of textile wastewaters by Gliding arc discharge plasma in the presence of $TiO_2$ catalyst, Journal of Hazardous Materials 164 (2009) 1266–1274.

[20] M.R. Ghezzar, M. Belhadj, F. Abdelmalek, A. Raïs, A. Addou, Non-thermal plasma degradation of wastewater in presence of titanium oxide by gliding arc discharge, International Journal of Environment and Waste Management 2 (2008) 458–470.

[21] F. Depenyou Jr., A. Doubla, S. Laminsi, D. Moussa, J.L. Brisset, J.-M. Le Breton, Corrosion resistance of AISI 1018 carbon steel in NaCl solution by plasma-chemical formation of a barrier layer, Corrosion Science 50 (2008) 1422–1432.

[22] J. Wang, J. Xiong, Q. Peng, H. Fan, Y. Wang, G. Li, B. Shen, Effects of DC plasma nitriding parameters on microstructure and properties of 304L stainless steel, Materials Characterization 60 (2009) 197–203.

[23] J.L. Brisset, D. Moussa, A. Doubla, E. Hnatiuc, B. Hnatiuc, G. Kamgang Youbi, J.M. Herry, M. Naïtali, M.-N. Bellon-Fontaine, Chemical reactivity of discharges and temporal post discharges in plasma treatment of aqueous media: examples of gliding arc discharge treated solutions, Industrial & Engineering Chemistry Research 47 (2008) 5761–5781.

[24] B. Benstaali, P. Boubert, B. Cheron, A. Addou, J.L. Brisset, Density and rotational temperature measurements of the NO and OH radicals produced by a gliding arc in humid air and their interaction with aqueous solutions, Plasma Chemistry and Plasma Processing 22 (2002) 553–571.

[25] R.A. Ruerhweinet, J.S. Hashman, J.W. Edwards, Chemical reactions of free radicals at low temperature, Journal of Physical Chemistry A 64 (1960) 1317–1322.

[26] L. Delair, J.L. Brisset, B. Cheron, Spectral, electrical and dynamic analysis of a 50 Hz air gliding arc, Journal of High Temperature Material Processes 5 (2001) 381–402.

[27] A. Imamura, K. Hirao, A molecular orbital approach to the eletrophilicity of H and •OH radical, Bulletin of the Chemical Society of Japan 52 (1979) 287–292.

[28] R. Peyrous, P. Pignolet, B. Held, Kinetic simulation of gaseous species created by an electrical discharge in dry or humid oxygen, Journal of Physics D: Applied Physics 22 (1989) 1658–1667.

[29] L.M. Dorfman, G.E. Adams, Reactivity of the hydroxyl radical in aqueous solution, National Standard Reference Data Series, National Bureau of Standard USA 46 (1973).

[30] H.C. Longuet-Higgins, C.A. McDowell, C.E.H. Bawn, A.S.C. Lawrence, O.S. Mills, General and physical chemistry, Annual Reports on the Progress of Chemistry 48 (1951) 7–86.

[31] E.J. Land, M. Ebert, Pulse radiolysis of aqueous phenol, Transactions of the Faraday Society 63 (1967) 1181–1190.

[32] J. Nahorny, D. Pagnon, M. Touzeau, Etude de la formation d'oxyde d'azote à partir des molécules excitées vibrationnellement, Internal report L. P. G. P., Universite' Paris- Sud, Orsay.

[33] G. Dorthe, Reactions of NO in the gas phase, in: Z. Alfassi (Ed.), N Centered Radicals, J. Wiley & Sons, Chichester, UK, 1998, pp. 1–38.

[34] J.O. Edwards, R.C. Plumb, The Chemistry of Peroxonitrites Progress in Inorganic Chemistry, J. Wiley & Sons, Chichester, UK, 1994, pp. 599–635.

[35] F. Moras, D. Seguin, B. Benstaali, A. Addou, B.G. Cheron, E. Hnatiuc, J.L. Brisset, Interaction between a non-thermal oxygenated plasma and aqueous solutions, in: Proceedings of International Conference HAKONE, 2000.

[36] R. Burlicaa, M.J. Kirkpatrickb, B.R. Lockeb, Formation of reactive species in gliding arc discharges with liquid water, Journal of Electrostatics 62 (2004) 309–321.

[37] A. Czernichowski, Gliding arc applications to engineering and environment control, Pure and Applied Chemistry 66 (6) (1994) 1301–1310.

[38] M.S. Anthelman, F.J. Harris Jr., The Encyclopedia of Chemical Electrode Potentials, Plenum Press, New-York, 1982.

[39] A.J. Bard, R. Parsons, J. Jordan, Standard Potentials in Aqueous Solution, IUPAC and M. Dekker, New-York, 1984.

[40] Collectif AFNOR, la qualité de l'eau, tome II, Analyses organoleptiques. Mesures physico-chimiques. Paramètres globaux. Composés organiques, NFT 90-102., Groupe Eyrolles S.A. AFNOR, 1999.

[41] D. Maron Molaem, G. Ingel, N. Brauner, Wettability and break-up of thin films on inclined surfaces with continuous and intermittent feed, Desalination 42 (1982) 87–96.

[42] N. Mhiri, Etude d'un procédé propre couplant l'absorption gaz/liquide microstructuré avec la distillation pour le traitement d'air chargé par composé organique volatil, 2005 (French thesis).

[43] J.H. Ryu, D.H. Choi, S.J. Kim, Numerical optimization of the thermal performance of a microchannel heat sink, International Journal of Heat and Mass Transfer 45 (2002) 2823–2827.

[44] M. Zanfir, A. Gavriilidis, Carbon dioxide absorption in a falling film microstructured reactor: experiments and modeling, Industrial & Engineering Chemistry Research 44 (2005) 1742–1751.

[45] E. Njoyim-Tamungang, P. Ghogomu, S. Laminsi, S. Nzali, A. Doubla, J.-L. Brisset, Coupling gliding discharge treatment and catalysis by oyster ll powder for pollution abatement of surface waters, Industrial & Engineering Chemistry Research 48 (2009) 9773–9780.

[46] F. Gnokam Zumgang, A. Doubla, J.-L. Brisset, Temporal post-discharge reactions in plasma-chemical degradation of slaughterhouse effluents, Chemical Engineering Communications 98 (2010) 483–493.

[47] I. Bouzaida, C. Ferronato, J.M. Chovelon, M.E. Rammahb, J.M. Herrmann, Heterogeneous photocatalytic degradation of the anthraquinonic dye, Acid Blue 25 (AB25): a kinetic approach, Journal of Photochemistry and Photobiology A 168 (2004) 23–30.

[48] E. Njoyim-Tamunganga, S. Laminsia, P. Ghogomua, D. Njopwouoa, J.-L. Brisset, Pollution control of surface waters by coupling gliding discharge treatment with incorporated oyster ll powder, Chemical Engineering Journal 173 (2011) 303–308.

[49] R.B. Bird, W.E. Stewart, E.N. Lightfoot, Transport Phenomena, Wiley International, Edition, 1960.

[50] D. Moussa, F. Abdelmalek, B. Benstaali, A. Addou, E. Hnatiuc, J.-L. Brisset, Acidity control of the oxidation reactions induced by non thermal plasma treatment of aqueous effluents in pollutant abatement processes, European Physical Journal: Applied Physics 29 (2005) 189–199.

[51] M. Saquib, M. Muneer, Photocatalytic degradation of CI Acid Green 25 and CI Acid Red 88 in aqueous suspensions of titanium dioxide, Coloration Technology 118 (2002) 307–315.

[52] A. Doubla, S. Laminsi, S. Nzali, E. Njoyim-Tamungang, J. Kamsu-Kom, J.-L. Brisset, Organic pollutants abatement and biodecontamination of brewery effluents by non-thermal plasma at atmospheric pressure, Chemosphere 69 (2007) 332–337.